

# Crystal structure of streptokinase $\beta$ -domain

Xiaoqiang Wang<sup>a</sup>, Jordan Tang<sup>b,c</sup>, Bret Hunter<sup>a</sup>, Xuejun C. Zhang<sup>a,\*</sup>

<sup>a</sup>Crystallography Program, Oklahoma Medical Research Foundation, 825 N.E. 13th Street, Oklahoma City, OK 73104, USA

<sup>b</sup>Protein Studies Program, Oklahoma Medical Research Foundation, 825 N.E. 13th Street, Oklahoma City, OK 73104, USA

<sup>c</sup>Department of Biochemistry and Molecular Biology, University of Oklahoma, Health Sciences Center, 940 Stanton L. Young Street, Oklahoma City, OK 73104-5042, USA

Received 24 August 1999

**Abstract** Streptokinase, a 47 kDa secreted protein of hemolytic strains of streptococci, is a human plasminogen activator and contains three structural domains linked by flexible loops. We describe here the crystal structure of the isolated streptokinase middle (SK $\beta$ ) domain determined at 2.4 Å resolution. Among the functionally important structural features is a putative binding site for a kringle domain of plasminogen located at the tip of a fully exposed hairpin loop. The distribution of genetically conserved residues of SK $\beta$  is strongly correlated with their functions. The extensive interface of the SK $\beta$  dimer suggests that such dimers may also exist in solution for free SK $\beta$ .

© 1999 Federation of European Biochemical Societies.

**Key words:** Streptokinase; Plasminogen;  $\beta$ -Grasp folding; Crystal structure

## 1. Introduction

Streptokinase (SK) is a plasminogen activator secreted by hemolytic strains of streptococci. SK converts human plasminogen to plasmin, a key fibrinolytic enzyme which degrades fibrin and dissolves blood clots [1,2]. Clinically, SK is widely used as a thrombolytic agent in the treatment of acute myocardial infarction following coronary thrombosis [3]. SK is also used by virulent strains of streptococci to activate bacterial bound plasminogen to plasmin, whose broad substrate specificity is utilized for penetrating the host tissues [4]. Human plasminogen (791 amino acid residues) contains seven structural domains, including the amino-terminal pre-activation domain, five kringle domains and the carboxy-terminal serine-protease catalytic domain [1]. Its activation peptide bond is located within the catalytic domain between Arg561 and Ser562, the hydrolysis of which confers proteolytic activity of plasmin. Unlike the physiological plasminogen activators, i.e. tissue-type plasminogen activator and urokinase, SK does not possess a proteolytic activity for the cleavage activation of plasminogen. Instead, SK forms a 1:1 stoichiometric complex with a plasminogen or a plasmin molecule. The active site of either plasminogen or plasmin in the complex catalyzes the hydrolysis of the activation peptide bond in free plasminogen molecules and converts them to plasmin [5].

The three-dimensional structure of the complex between

group C SK (414 residues) and the catalytic domain of human plasmin (micro-plasmin,  $\mu$ Pm) has recently been determined at 2.9 Å resolution using X-ray crystallography [6]. Since this complex is believed to be the functional core of the SK-plasmin activator complex [7], many functional interpretations of the SK mechanism were derived from this structure. The crystal structure reveals that SK contains three sequential domains of roughly equal sizes, namely  $\alpha$ ,  $\beta$  and  $\gamma$  domains from the amino- to the carboxy-termini, linked by flexible loops. These three domains surround  $\mu$ Pm to form a concave-shaped complex with the plasmin active site located at the bottom of the concavity. The SK  $\alpha$  domain (SK $\alpha$ , residues 1–146) is structurally and functionally homologous to another bacterial plasminogen activator, staphylokinase (SAK, 136 residues), from staphylococci [8] and binds near the active site of plasmin(ogen). The  $\alpha$  domain renders additional recognition surface for substrate plasminogen to interact with, thus endowing the complex with a plasminogen activator activity which is not found in plasmin itself. The SK  $\gamma$  domain (SK $\gamma$ , residues 291–414) binds to plasminogen near the region of the activation bond, implying its function in the contact activation of plasminogen by SK [6]. In the SK- $\mu$ Pm complex crystal structure, the SK  $\beta$  domain (SK $\beta$ , residues 147–290) contributes substantially to the overall shape of the putative substrate binding concave of the complex [6], suggesting that SK $\beta$  may also be involved in the recognition of substrate plasminogen. This is supported by an earlier mutagenesis experiment that two consecutive lysine residues, Lys256 and Lys257, located within SK $\beta$  were shown to be intimately involved in the substrate binding [9], possibly involving one of the lysine binding kringles of plasminogen [10]. A synthetic fragment from SK $\beta$ , residues 254–273, showed marked inhibition to plasminogen activation by the SK-plasminogen complex, whereas it could not inhibit amidolytic activity of plasmin, suggesting that this region may be directly involved in binding to substrate plasminogen [11]. Furthermore, it was shown that an isolated SK $\beta$  can tightly bind to native plasminogen ( $K_d \sim 10^{-8}$  M) [12]. Such a strong affinity of SK $\beta$  with plasmin(ogen) is inconsistent with the structural evidence of meager contacts between SK $\beta$  and  $\mu$ Pm in the activator complex, suggesting that the substrate plasminogen may be a target of SK $\beta$ .

The above discussion serves to illustrate that the structure of SK $\beta$  is important for fully understanding the mechanism of plasminogen activation by SK. In the complex crystal structure SK $\beta$  was the most mobile domain, reflected by its rather high average temperature factor ( $80 \text{ Å}^2$ ) [6]. In addition, the SK molecule was cleaved between Lys257 and Ser258 within SK $\beta$ , which rendered the corresponding region disordered in the complex crystal. To overcome these obstacles, we have undertaken the determination of the free SK $\beta$  domain itself.

\*Corresponding author. Fax: (1) (405) 271-3980.  
E-mail: zhangxc@omrf.ouhsc.edu

**Abbreviations:** SK, streptokinase; SK $\alpha$ , SK $\beta$ , and SK $\gamma$ , the amino-terminal, middle and carboxy-terminal domains of streptokinase; SAK, staphylokinase;  $\mu$ Pm, micro-plasmin, i.e. the catalytic domain of plasmin

Here we report a 2.4 Å resolution crystal structure of the isolated SK  $\beta$  domain in which the peptide is intact throughout the entire domain. Thus, this crystal structure presents a SK $\beta$  model of higher resolution than the previous SK- $\mu$ Pm structure for studying the functions of the SK-plasminogen system.

## 2. Materials and methods

### 2.1. Protein purification and crystallization

Recombinant SK $\beta$  (residues 147–290) was constructed by splicing previously cloned SK gene from group C *Streptococcus equisimilis* [6] and expressed from a pET11 vector (Novagen, Madison, WI) with *Escherichia coli* strain BL21 as the host. The protein was expressed as ‘inclusion bodies’ and was refolded using the rapid dilution method [13]. Purification was carried out with a Sephacryl S-300 column followed by a FPLC Resource Q ion-exchange column using a buffer containing 20 mM Tris (pH 8.0), 400 mM urea, and a gradient of 0.0–1.0 M NaCl. Initial crystallization conditions were obtained using crystal screening kits from Hampton Research (Laguna Niguel, CA). The crystal used for data collection was grown at 20°C from a sitting drop of 1:1 mixture of the protein sample (30 mg/ml) and a reservoir solution containing 25% (w/v) polyethylene glycol (PEG) 6000, 100 mM  $(\text{NH}_4)_2\text{SO}_4$ , 100 mM  $\text{MgCl}_2$  and 100 mM 2-(*N*-morpholino) ethanesulfonic acid (MES) (pH 5.5). Crystals grew to full size ( $0.4 \times 0.4 \times 0.04 \text{ mm}^3$ ) in about 2 weeks. The crystal was equilibrated with 36% (w/v) PEG 6000, 100 mM MES (pH 5.5) before being flash-frozen to approximately  $-180^\circ\text{C}$  in a nitrogen gas stream for data collection.

### 2.2. Crystallography studies

X-ray diffraction data were collected with a RAXIS-II image plate system and were processed with the program suite HKL [14]. The crystal diffracted to 2.4 Å (see Table 1 for more statistics).

The crystal form belongs to space group  $\text{P}2_12_12_1$ . The map of Patterson function calculated with the observed data (2.4 Å) showed one 30-standard-deviation peak (corresponding to  $\sim 30\%$  of the intensity of the origin peak) at the fractional position of (0.00, 0.05, 0.50), indicating a local translation along that direction. The phases of X-ray diffractions were determined by molecular replacement (MR) methods with the program AMoRe [15] and a search model derived from the corresponding part of our 2.9 Å resolution crystal structure of the SK- $\mu$ Pm complex [6]. One crystallographic asymmetric unit contains four molecules of SK $\beta$  with a 49% solvent content. The initial *R*-factor of the MR solution is 0.50 (20.0–3.0 Å). Density modification, including solvent flattening and non-crystallographic averaging, was carried out with the program DM [16]. The resulting electron density map was improved particularly in previously disordered regions [6], allowing the peptide backbone to be built continuously. Interactive model building with the program O [17] and crystallography refinement with the program CNS [18] were carried out iteratively. Non-crystallographic symmetry restriction and restrained indi-

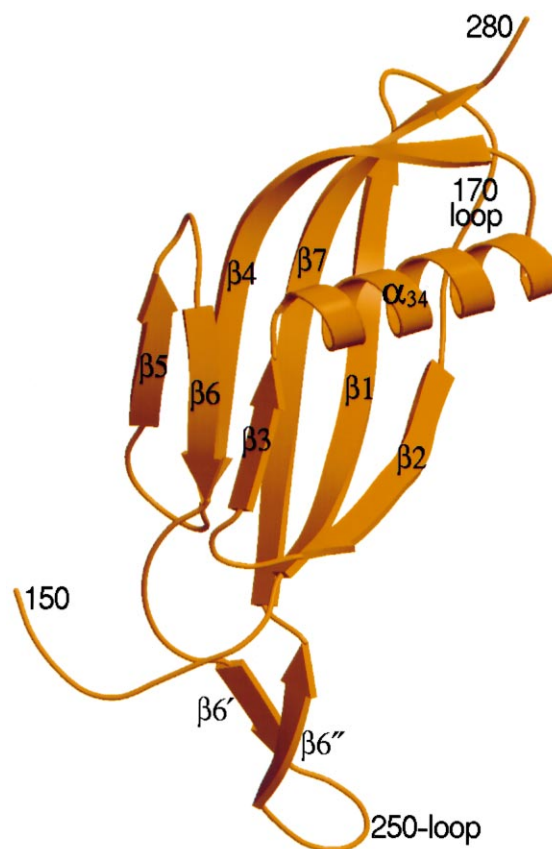


Fig. 1. Ribbon diagram of the overall folding of streptokinase  $\beta$  domain. The overall secondary structure assignment is consistent with that of the SK- $\mu$ Pm complex:  $\beta_1$  = 158–169,  $\beta_2$  = 183–188,  $\beta_3$  = 192–195,  $\beta_4$  = 214–226,  $\beta_5$  = 232–236,  $\beta_6$  = 241–245,  $\beta_6'$  = 251–255,  $\beta_6''$  = 260–264, and  $\beta_7$  = 266–278; between strands  $\beta_3$  and  $\beta_4$  is the only  $\alpha$ -helix in SK $\beta$ ,  $\alpha_{3.4}$  = 196–210. This figure was drawn with the programs Molscript [29] and Raster3D [30].

vidual temperature-factor refinement were applied at the initial stage of refinement. A bulk solvent correction and an anisotropic overall temperature-factor refinement were applied at the final stage of the refinement. No backbone  $\phi$ - $\psi$  torsion angle pair was located in a disallowed region of the Ramachandra plot, and more than 85% residues were in the energetically most favored regions, as defined in PROCHECK [19].

## 3. Results and discussion

### 3.1. Structural description

A crystal structure has been determined at 2.4 Å resolution for the  $\beta$  domain of recombinant SK, encompassing residues 147–290 of the native SK. Phases of the X-ray diffractions were obtained using molecular replacement methods. There are four SK $\beta$  molecules per crystallographic asymmetric unit. The structure has been refined to an *R*-factor of 0.24 with an *R*<sub>free</sub> of 0.30 [20].

The overall folding of SK $\beta$  belongs to the  $\beta$ -grasp folding family [21]. Like a typical protein in this family, SK $\beta$  contains a single  $\alpha$ -helix ( $\alpha_{3.4}$ ) packed against a five-stranded  $\beta$ -sheet ( $\beta_2$ ,  $\beta_1$ ,  $\beta_7$ ,  $\beta_4$  and  $\beta_5$ ) (Fig. 1). The topology of this major  $\beta$ -sheet is (–1, +3x, +1, –2x) [22]. A short two-stranded  $\beta$ -sheet ( $\beta_3$  and  $\beta_6$ ) packs on the same side of the major  $\beta$ -sheet as the  $\alpha$ -helix. The other side of the major  $\beta$ -sheet is essentially flat albeit twisted, which in the SK- $\mu$ Pm structure contributed

Table 1  
Data collection and refinement statistics

Data statistics	
Space group	$\text{P}2_12_12_1$
Unit cell	$a = 74.0 \text{ Å}$ $b = 84.0 \text{ Å}$ $c = 97.2 \text{ Å}$
Resolution (Å)	19.8–2.4
<i>R</i> <sub>merge</sub> (%)	0.079 (0.279)
Number of reflections	23 859
Completeness (%)	98.1
Refinement statistics	
<i>R</i> <sub>working</sub> (%)	23.9
<i>R</i> <sub>free</sub> (%)	30.0
rms deviation from ideal values	
bond length (Å)	0.009
bond angle (°)	1.60
Average temperature factor (Å <sup>2</sup> )	

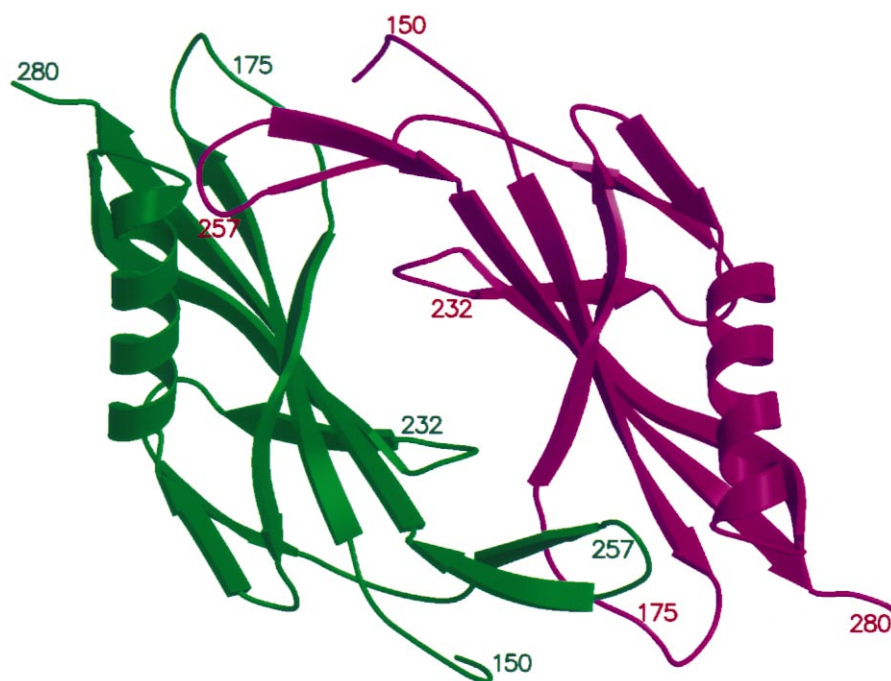


Fig. 2. Stereo view of a ribbon diagram of the primary SK $\beta$  dimer. This figure was drawn with the programs Molscript [29] and Raster3D [30]

part of the putative substrate binding concave. Additionally, a hairpin loop (250-loop, residues 251–264), including strands  $\beta_6'$  and  $\beta_6''$ , protrudes into the solvent and bends to the opposite side of the major  $\beta$ -sheet from the  $\alpha$ -helix. Between strands  $\beta_1$  and  $\beta_2$ , residues 170–182 form the 170-loop which accommodates three consecutive aspartate residues and other charged residues. Like other  $\beta$ -grasp folding proteins, SK $\beta$  possesses a hydrophobic core between the major  $\beta$ -sheet and the  $\alpha$ -helix. Two buried salt bridges, Arg219-Glu272 and Arg248-Asp268, which are conserved in SK $\beta$  among the SK family [23], are entrenched in the core and are likely to contribute to the structure stability.

The current crystal structure illustrates that the SK  $\beta$  domain has a rigid overall structure. The four copies of SK $\beta$  molecules in an asymmetric unit, designated A–D, are essentially identical and are similar to that in the SK- $\mu$ Pm complex. For the four molecules, the root mean square (rms) deviation of  $C_\alpha$  atoms (of residues 150–169, 183–250, and 165–280) ranges from 0.36 to 0.66 Å. Similarly, the rms deviation for the same set of atoms between the four molecules and the SK  $\beta$  domain in the complex crystal structure ranges from 0.75 to 0.90 Å; the statistical significance of these differences is uncertain because of the high mobility of the SK  $\beta$  domain in the complex structure. In the refined model, residues 149–285 are seen in SK $\beta$  molecules A and B while residues 149–280 are visible in molecules C and D. The amino-terminal two residues and carboxy-terminal five/ten residues are disordered in this crystal form, albeit they were visible in the SK- $\mu$ Pm complex structure because of the peptide interactions to the neighboring domains.

### 3.2. Two mobile regions within SK $\beta$

The electron densities for the 170-loop and 250-loop were invisible in the SK- $\mu$ Pm complex crystal structure. In the current crystal form, they are clearer but still have higher than average temperature factors. The backbone average temper-

ature factors of the four SK $\beta$  molecules range from 52 to 72 Å<sup>2</sup> for the 170-loop and from 43 to 66 Å<sup>2</sup> for the 250-loop, compared with the overall one of 42 Å<sup>2</sup>.

Whereas the 250-loop was proteolytically cleaved between Lys257 and Ser258 in the complex structure [6], in the current crystal form this loop is intact and forms a hairpin structure with four hydrogen bonds between residues 251–264, 253–262 (two bonds), and 255–260. This loop is hydrophilic in general and contains three glutamate residues at the stem and two lysine residues at the tip. It is distal from the interface between SK $\beta$  and  $\mu$ Pm in the SK- $\mu$ Pm complex, suggesting that this loop is unlikely to have a direct role in the formation of the SK-plasmin(ogen) complex. The side chain conformation of the two functionally important lysine residues [9] is poorly defined in the electron density map, indicating that they are unimportant for the structural stability. This loop is also one of the early proteolytic digestion sites in SK [6,24], therefore its conformational integrity is perhaps not functionally important. Since there is no direct evidence on the binding site of the 250-loop to plasminogen, computer modeling based on the SK- $\mu$ Pm crystal structure and other available information including the position of a substrate-like  $\mu$ Pm relative to a plasminogen activator [8] was carried out to search possible targets of the 250-loop. The result (data not shown) suggests that it is feasible to dock the kringle-5 of human plasminogen in such a way that its lysine binding site is in the vicinity of lysine residues at the tip of the SK $\beta$  250-loop while its carboxy-terminus connects to the amino-terminus of the substrate-like  $\mu$ Pm.

The 170-loop is located on the edge of the major  $\beta$ -sheet, preceding the strand  $\beta_2$ . It runs more or less antiparallel to its  $\beta_1$  neighboring strand, but there is no hydrogen bond network between this loop and  $\beta_1$ . Although this loop region was mobile in the SK- $\mu$ Pm complex, its relative location to the putative substrate binding site suggests its importance in the interaction with substrate plasminogen. The highly exposed

position of this loop and its flexible conformation would explain its significant involvement in the immunogenicity of SK [25] and its possible induced-conformational change upon binding to a substrate.

### 3.3. Crystal packing

The four copies of SK $\beta$  in an asymmetric unit form two dimers (A–C and B–D) with both local two-fold axes approximately parallel to the *b* axis of the unit cell. The two primary dimers share the same dimer interface and are further related to each other by the local translation shown in the native Patterson function (or by an equivalent dyad symmetry with the local two-fold axis parallel to the *c* axis of the unit cell).

The overall shape of the primary dimer resembles a donut, with each monomer contributing half of the ring (Fig. 2). The flat sides of the major  $\beta$ -sheets of the two monomers face each other, with their  $\beta$  strands running parallel to the plane of the donut ring. The dimer interface is extensive and complementary. Each dimer buries  $\sim 2750$  Å<sup>2</sup> surface area from the two monomers. One major interaction involves the coverage of the 170-loop from one monomer by the 250-loop from the other. Within this interaction are, for example, a pair of backbone hydrogen bonds flanking residues 178<sub>A</sub> and 252<sub>C</sub>, a salt bridge between Lys180<sub>A</sub> and Glu253<sub>C</sub> and a cluster of hydrophobic side chains from both monomers. Another major interaction, located at the bottom center of the donut, involves loops between  $\beta_4$  and  $\beta_5$  (residues 223–234) from both monomers. The guanidine groups of the two Arg232 residues stack to each other while hydrogen bonding to the backbone carbonyl oxygen of residues 230 from their partner monomers. Surrounding them is a hydrophobic ring formed by Ile223, Ile230, Phe231 and Ile234 from both monomers. Most of these hydrophobic residues are involved in the SK $\beta$ –SK $\alpha$  interface in the SK– $\mu$ Pm complex and would become solvent-exposed in a free SK $\beta$  monomer. Although dimerization of SK $\beta$ -like proteolytic fragments of SK was suspected to exist in solution [26], there has been no evidence suggesting that dimerization plays a role in SK function. Stereochemically, it is possible that this primary dimerization exists between the  $\beta$  domains of native SK; but it could not occur between two SK-plasmin(ogen) complexes because of severe structural overlaps.

The secondary dyad symmetry relating the two primary dimers in the asymmetric unit involves mainly the two  $\beta_5$

strands (residues 231–238) from monomers A and B, part of which also participate in the above mentioned hydrophobic ring within the primary dimer. While the major  $\beta$ -sheets of monomers A and B appear forming one extended  $\beta$ -sheet, their interface is actually stabilized by a hydrophobic side chain zipper (Met237<sub>A</sub>, Ile234<sub>B</sub>, Ile234<sub>A</sub> and Met237<sub>B</sub>) rather than by main chain hydrogen bonds between the two  $\beta_5$  strands. A pair of salt bridges (Arg232<sub>A,B</sub>–Asp238<sub>B,A</sub>) flank the hydrophobic zipper. This secondary dimerization buries  $\sim 2700$  Å<sup>2</sup> surface area from the two primary dimers.

### 3.4. Structural homology

Among the three  $\beta$ -grasp folding domains of SK, the three-dimensional structural similarity between SK $\alpha$  and SK $\beta$  is the most clear. The rms deviation is 0.6 Å for 90 pairs of C $\alpha$  atoms between them selected using a 1.0 Å distance cutoff during optimal superposition. In addition, SAK also shares the same  $\beta$ -grasp folding with these two SK domains. Sequence homology between these protein domains is beyond recognition using conventional sequence alignment methods. However, using a three-dimensional structure-based sequence alignment we recognize some similarity among these domains (Fig. 3). The validity of this alignment is reinforced by its correlation with the functions of these domains, i.e. SK $\alpha$  and SAK perform similar functions in a plasminogen activator complex [6,8] while SK $\beta$  does not. For example, SAK Glu46 and SK $\alpha$  Glu39 are found to be critical for interacting with plasminogen Arg719 in the complex formation; however, their topologically equivalent position (residue 185) in SK $\beta$  has a leucine residue which would abolish the favorable electrostatic interaction. Such detailed structural discrepancies would explain the observation that SK $\beta$  and SAK do not compete for human plasminogen to form complexes [27]. Since it forms a  $10^{-8}$  M  $K_d$  complex with plasminogen, SK $\beta$  is most likely to target plasminogen regions different from where SK $\alpha$  and SAK bind to, even in the absence of them.

Genetic analysis of SK from different strains of streptococci has demonstrated that SK as a group of plasminogen activators are heterogeneous [23]. Combined with the knowledge of the three-dimensional structure of SK from group C streptococci, sequence analysis clearly shows that most streptokinases consist of a three-sequential-domain structure, and that SK $\beta$  is the most variable domain in term of its primary

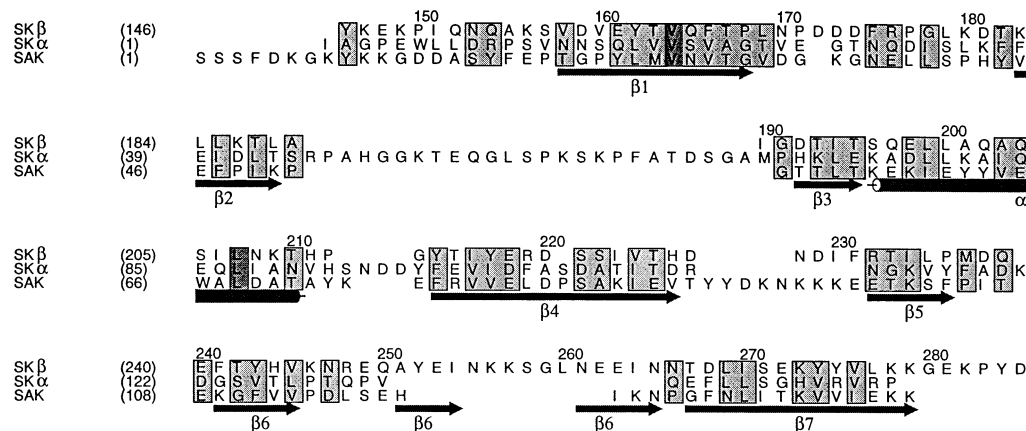


Fig. 3. Amino acid sequence alignment of SK $\beta$ , SK $\alpha$  and SAK based on their three-dimensional structural homology. Conserved residues are highlighted. This figure was produced using the program ALSCRIPT [31].

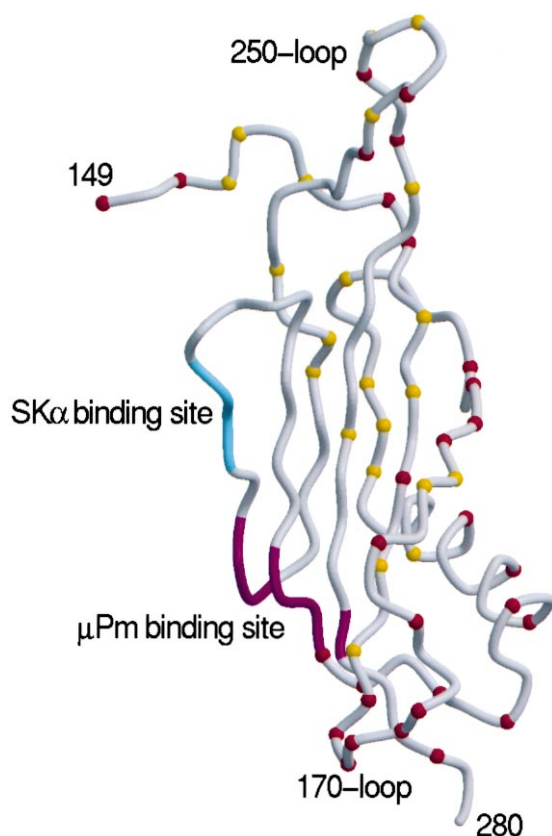


Fig. 4. Distribution of variable residues [23] in SK $\beta$ . The conservative variations are marked with yellow dots, and non-conservative ones are marked in red. The regions binding to SK $\alpha$  and  $\mu$ Pm are highlighted in blue and magenta, respectively. The orientation of the molecule is different from that in Fig. 1 by a  $\sim 180^\circ$  rotation about a horizontal axis. This figure was drawn with the programs Molscrip [29] and Raster3D [30].

sequence [23]. Mapping of the variable residues on the current structure of SK $\beta$  shows that most of the mutations occur on the surface of the three-dimensional structure, including the solvent-exposed side of the strand  $\beta_1$ , 170-loop, solvent-exposed side of the long  $\alpha$ -helix with its following loop and 250-loop (Fig. 4). They are distributed on both sides of the major  $\beta$ -sheet but away from the interfaces of both SK $\beta$ -SK $\alpha$  and SK $\beta$ - $\mu$ Pm in general. A subgroup of SK from *Streptococcus uberis* isolated from bovine was found to contain the  $\alpha$  and  $\beta$  domains only [28], suggesting the essential roles of these two domains in pathogenic invasion.

**Acknowledgements:** We thank Dr. A. Bochkarev of Department of Biochemistry and Molecular Biology, University of Oklahoma Health Sciences Center for helping in data collection. This work is supported by NIH Grant HL 60626.

## References

- [1] Bachmann, F. (1994) in: Hemostasis and Thrombosis: Basic Principles and Clinical Practice (Coleman, R.W., Hirsh, J., Marder, V.J. and Salzman, E.W., Eds.), pp. 1592–1622, J.B. Lippincott, Philadelphia, PA.
- [2] Collen, D. and Lijnen, H.R. (1995) Thromb. Haemost. 74, 167–171.
- [3] Gulba, D.C., Bode, C., Runge, M.S. and Bubber, K. (1996) Ann. Hematol. 73, S9–27.
- [4] Brodder, C.C., Lottenberg, R., von Mering, G.O., Johnston, K.H. and Boyle, M.D. (1991) J. Biol. Chem. 266, 4922–4928.
- [5] Castellino, F.J. (1979) Trends Biochem. Sci. 4, 1–5.
- [6] Wang, X.Q., Lin, X.L., Loy, J.A., Tang, J. and Zhang, X. (1998) Science 281, 1662–1665.
- [7] Summaria, L. and Robbins, K.C. (1976) J. Biol. Chem. 251, 5810–5813.
- [8] Parry, M.A.A., Fernandez-Ctalan, C., Bergner, A., Huber, R., Hopfner, K., Schlott, B., Guhrs, K. and Bode, W. (1998) Nature Struct. Biol. 5, 917–923.
- [9] Lin, L.-F., Oeun, S., Hough, A. and Reed, G.L. (1996) Biochemistry 35, 16879–16885.
- [10] Chang, Y., Mochalkin, I., McCance, S.G., Cheng, B., Tulinsky, A. and Castellino, F.J. (1998) Biochemistry 37, 3258–3271.
- [11] Nihalani, D., Raghava, G.P. and Sahni, G. (1997) Protein Sci. 6, 1284–1292.
- [12] Rodriguez, P., Fuentes, P., Barro, M., Alvarez, J.G., Munoz, E., Collen, D. and Lijnen, H.R. (1995) Eur. J. Biochem. 229, 83–90.
- [13] Lin, X.L., Lin, Y.Z. and Tang, J. (1994) Methods Enzymol. 241, 195–224.
- [14] Otwinowski, Z. and Minor, W. (1997) Methods Enzymol. 276, 307–326.
- [15] Navaza, J. (1994) Acta Crystallogr. A50, 157–163.
- [16] Cowtan, K.D. and Main, P. (1996) Acta Crystallogr. D52, 43–48.
- [17] Jones, T.A., Zou, J.Y., Cowan, S.W. and Kjeldgaard, M. (1991) Acta Crystallogr. A47, 110–119.
- [18] Brünger, A.T. et al. (1998) Acta Crystallogr. D54, 905–921.
- [19] Laskowski, R.A., MacArthur, M.W., Moss, D.S. and Thornton, J.M. (1993) J. Appl. Crystallogr. 26, 283–291.
- [20] Brünger, A.T. (1992) Nature 355, 472–474.
- [21] Murzin, A.G., et al. Chothia, C. (1995) J. Mol. Biol. 247, 536–540.
- [22] Richardson, J.S., Richardson, D.C. and Thomas, K.A. (1976) J. Mol. Biol. 102, 221–235.
- [23] Malke, H. (1993) Zbl. Bakteriell. 278, 246–257.
- [24] Young, K.-C., Shi, G.-Y., Chang, Y.-F., Chang, B.-I., Chang, L.-C., Lai, M.-D., Chung, W.-J. and Wu, H.-L. (1995) J. Biol. Chem. 270, 29601–29606.
- [25] Torrents, I., Reyes, O., Ojalvo, A.G., Seralena, A., Chinea, G., Cruz, L.J. and Fuente, J. (1999) Biochem. Biophys. Res. Commun. 259, 162–168.
- [26] Rodriguez, P. et al. (1994) Fibrinolysis 8, 276–285.
- [27] Rodriguez, P., Collen, D. and Lijnen, H.R. (1995) Fibrinolysis 9, 298–303.
- [28] Lincoln, R.A. and Leigh, J.A. (1997) in: Streptococci and the Host (Heraud, Ed.), Plenum Press, New York.
- [29] Kraulis, P.J. (1991) J. Appl. Crystallogr. 24, 946–950.
- [30] Merritt, E.A. and Murphy, M.E.P. (1994) Acta Crystallogr. D50, 869–873.
- [31] Barton, G.J. (1993) Protein Eng. 6, 37–40.